Journal of Hydrology 572 (2019) 160–168

Contents lists available at ScienceDirect

Journal of Hydrology

journal homepage: www.elsevier.com/locate/jhydrol

Research papers

Impacts of urban water consumption under climate change: An adaptation measure of rainwater harvesting system

Chia-Chun Lin[a], Kuan-Yu Liou[a], Mengshan Lee[a,b], Pei-Te Chiueh[a,*]

[a] Graduate Institute of Environmental Engineering, National Taiwan University, No. 71, Chou-Shan Rd., Da'an Dist., Taipei City 106, Taiwan
[b] Department of Safety, Health and Environmental Engineering, National Kaohsiung University of Science and Technology, No. 1, University Rd., Yanchao Dist., Kaohsiung City 824, Taiwan

ARTICLE INFO

This manuscript was handled by G. Syme, Editor-in-Chief, with the assistance of Giorgio Mannina, Associate Editor

Keywords:
Water consumption impacts
Dynamic characterization factors
Soil and Water Assessment Tool (SWAT)
Urban water system

ABSTRACT

Understanding the environmental impacts associated with water-related adaptation measures plays an important role in decision making, as some adaptation measures may not offer environmental benefits compared to traditional water systems. The water depletion index (WDI) is one water stress indicator used to estimate the impacts of water consumption. A dynamic WDI was constructed and employed in this study under climate change scenarios with weather and streamflow modeling. To demonstrate whether adaptation measures can reduce water depletion and to demonstrate how dynamic WDI affects assessment results, Taipei, a highly developed and populated city in Taiwan, was selected as a case study site. Decreased WDI from July to August and increased WDI from September to October were simulated under climate change. This approach implied that when measuring water consumption impacts, the WDI should be applied according to the corresponding time period. Additionally, by substituting 70% of potable water with rainwater in a four-story building, 17.9–159.3 m^3 of the freshwater depletion risk might be reduced every month. As adaptation measures can be long-term strategies and long-lasting infrastructures, a dynamic WDI could provide policy makers with a method to accurately and effectively assess the impacts of applying water-related adaptation measures in response to climate change.

1. Introduction

Water crises have been identified as one of the greatest global challenges of the next 10 years (The World Economic Forum, 2016). According to the Fifth Assessment Report (AR5) of the Intergovernmental Panel on Climate Change (IPCC), extreme weather events such as rainstorms and droughts are increasing, particularly due to rainfalls that are inconsistent and unpredictable, both spatially and temporally (IPCC, 2014). Studies have also suggested that by 2025, these extreme weather events may result in elevated water stress in the form of an increased freshwater withdrawal-to-availability ratio in several countries (UNEP, 2008).

Adaptation in response to future extreme water stress is necessary to reduce the impact of oncoming water crises. Recently, the concept of the sponge city was proposed as an adaptation measure to improve water resilience at the urban level (Liu et al., 2015). This concept can be implemented using such measures as a rainwater harvesting system (RWHS) (Pandey et al., 2003), which enables the recycling and reuse of runoff and provides the additional benefit of runoff reduction (Sample and Liu, 2014). However, a drawback of this system is its high energy consumption, which may limit its environmental feasibility in practice (Vieira et al., 2014). A study on potable water savings using RWHS showed a reduction of up to 11% of total water consumption in Paris (Belmeziti et al., 2014). An annual water savings potential of up to 46,500 L per household was also estimated using an optimized tank (Fonseca et al., 2017). Recent studies have therefore recommended understanding the impacts of these conservation systems from a life cycle perspective (Anand and Apul, 2011; Godskesen et al., 2013; Li et al., 2018) in order to provide a comprehensive evaluation of the benefits and trade-offs of water-related adaptations.

Various approaches to measuring the consequences of water consumption have been proposed recently (Berger et al., 2014; Pfister et al., 2009). Water stress indicators have been used as characterization factors in quantifying the causality between water consumption and its related impacts on water resources (Berger et al., 2014; Pfister et al., 2009). Temporal and spatial conditions at the points of water consumption are critical to improve the accuracy of the impact assessments (Núñez et al., 2015; Scherer et al., 2015; Soligno et al., 2017). Hoekstra

* Corresponding author.
E-mail address: ptchueh@ntu.edu.tw (P.-T. Chiueh).

https://doi.org/10.1016/j.jhydrol.2019.02.032
Received 27 October 2018; Received in revised form 16 February 2019; Accepted 18 February 2019
Available online 27 February 2019

et al. (2012) and Pfister and Bayer (2014) noted that the high variability of water availability in a given year can be a challenge to efficient water resource management and indicated that monthly resolution can reveal water stress more accurately. Moreover, the impacts of water consumption depend on the status of water environments, which may vary by region or time period (Núñez et al., 2015). Because long-term weather conditions determine water environments and water availability (Núñez et al., 2015), impacts can differ depending on the time period. Therefore, it is suggested that water demand as well as water availability for the specific location and time period should be considered when assessing future water consumption impacts.

This study constructed a monthly dynamic water depletion index (WDI_{mon}) with improved temporal and spatial resolution under consideration of climate change. The impacts of urban water consumption, defined as the risk of monthly freshwater depletion (RFD_{mon}), was derived from direct and indirect water consumption and the region-specific WDI_{mon}. To demonstrate the application of the dynamic WDI_{mon} in impact assessments of urban water consumption, Taipei, the capital city of Taiwan, was chosen as a case study site. An RWHS in a building was designed to show the potential impacts of adaptation measures with RFD_{mon} results. The dynamic WDI_{mon} approach could be of interest to researchers or policy makers in determining long-term water management policies that consider the influences of climate change.

2. Methods

2.1. Monthly water depletion index (WDI_{mon})

The WDI proposed in this study was adopted from Berger et al. (2014) to evaluate the depletion of freshwater resources due to water consumption. The monthly WDI (WDI_{mon}, dimensionless) reflecting temporal-scale modifications can be calculated using Eqs. (1) and (2) as follows:

$$WDI_{mon} = \frac{1}{1 + (\frac{1}{0.01} - 1) \times e^{-AF_{ERF,mon} \times CTA^{*}_{mon}}} \quad (1)$$

$$\mathrm{CTA}^{*}_{mon} = \frac{C_{mon}}{A_{mon} + SWS_{mon}} \times AF_{GWS,mon} \quad (2)$$

$$\mathrm{SWS}_{mon} = \sum_{h} (V_{dam,mon,h}) + \sum_{k} (A_{lake/wetland,k} \times d_{eff,mon,k}) \quad (3)$$

where WDI_{mon} is adjusted from a logistic function with an ecological reference flow-adjusted factor ($AF_{ERF,mon}$,dimensionless) and the monthly water consumption-to-availability ratio (CTA^{*}_{mon}, dimensionless, given by Eq. (2)) to obtain continuous values ranging from 0.01 to 1 (Berger et al., 2014; Pfister et al., 2009). C_{mon} is the monthly water consumption of the research area in m^3/month (see Section 2.1.1 Monthly water consumption); A_{mon} is the monthly water availability in m^3/month (see Section 2.1.2 Available water estimation); SWS_{mon} is the monthly usable surface water stocks in m^3/month (given by Eq. (3)); $AF_{GWS,mon}$ is the monthly groundwater stocks adjusted factor; and 0.9 was applied in this study to indicate that the geological structure of the research area is a major groundwater basin with > 300 mm annual recharge which can reduce 10.0% freshwater scarcity (Berger et al., 2014).

As CTA^{*}_{mon} exceeds 0.80, WDI_{mon} climbs to 1, indicating severe water stress (as shown in supporting information Fig. S1). Table S1 shows the determination of $AF_{ERF,mon}$ based on the monthly average stream flow and monthly 95th percentile exceedance flow (Q95), which was defined as the ecological reference flow (ERF) (Acreman et al., 2008; Taiwan Water Resources Agency, 2014). $AF_{ERF,mon}$ with the value 12.5 means that the Q95-to-monthly average stream flow ratio is less than 0.2.

SWS_{mon} was calculated using the monthly inflow of the dam h ($V_{dam,mon,h}$, m^3/month) and the usable volume of lake/wetland k, which were estimated at the surface area ($A_{lake/wetland,k}$, m^2) and multiplied by the monthly effective depth ($d_{eff,mon,k}$, m/month). In the case study, the $V_{dam,mon,h}$ was derived by annual inflow to the dam because of data availability and the $d_{eff,mon,k}$ was set to be 0 as a result of no lake and wetland in the watershed.

2.1.1. Monthly water consumption (C_{mon})

Projection of water consumption in the research area of this study mainly focuses on municipal water demand or water supply for domestic purposes. Thus, future monthly water consumption was estimated based on two sources: (1) domestic water consumption (Eq. (4)) and (2) other municipal water use. Monthly domestic water consumption ($WCon_{Domestic,mon}$, m^3/month) was calculated based on future population projections ($Pop_{Proj.}$, capital) with some assumptions: the population-served ratio (PopServed%, dimensionless) reaches 100% in the future; water consumption per capita per day ($WCon_{lpcd}$, lpcd) remains as it is at present, which is 327 L, and revenue water ratio (RevenueW%, dimensionless) slightly increases to 80% in the future (Table S2).

$$WCon_{Domestic,mon} = (\mathrm{Pop}_{Proj.} \times \mathrm{PopServed\%} \times \mathrm{WCon}_{lpcd} \times days/month \times 1/1000) \div \mathrm{RevenueW\%} \quad (4)$$

Other municipal water use was determined based on historically distributed water quantity in 2009–2012 with monthly variation. The quantity of other municipal water use was assumed to be the same in the future time periods.

2.1.2. Monthly available water estimation (A_{mon})

Monthly available water in the future time periods considered in this study was derived by TaiWAP for future weather generation (with 1996–2015 as baseline years) (Liu et al., 2009; Tung et al., 2014) and using a hydrological model of a soil and water assessment tool (SWAT) for streamflow simulation (Neitsch et al., 2009). In TaiWAP, climate change scenarios were selected based on IPCC AR5: four Representative Concentrative Pathways (RCPs), RCP 2.6, RCP 4.5, RCP 6.0, and RCP 8.5, with four time periods, 2021–2040 (2030s), 2041–2060 (2050s), 2061–2080 (2070s) and 2081–2100 (2090s) (IPCC, 2014). Two General Circulation Models (GCMs), CCSM4 and CSIRO-Mk3.6.0 models, were chosen because they were suitable for Taiwan according to the rankings by Tung et al. (2014). The resolution of weather projections for regional simulation was downscaled from 300 km to 5 km in TaiWAP through statistical approaches (Hsu et al., 2011).

The SWAT model, which was originally a watershed and subbasin level simulations model, was utilized to simulate water availability as streamflow for estimating water stress indicator (Scherer et al., 2015). The ArcSWAT 2012 model was applied in this study to enhance spatial resolution and to assess water consumption impacts. Streamflow calibration was based on daily observed data from 2009 to 2010 and validation from 2011 to 2012 (Fig. S2). Manual calibration was done according to the parameters that govern the hydrologic process (Table S3). The performance of SWAT was evaluated by three statistics: the Nash-Sutcliffe efficiency (NSE), standard deviation ratio (RSR), and coefficient of determination (R^2). If NSE > 0.5, RSR < 0.7, and R^2 > 0.5, the performance was confirmed as satisfactory (Moriasi et al., 2007). The goodness of fit is shown in Table S4.

2.2. Assessing the risk of monthly freshwater depletion (RFD_{mon})

The risk of monthly freshwater depletion (RFD_{mon}, m^3/month) is used to represent the potential consequences of water consumption in the watersheds (Berger et al., 2014), which can be quantified by multiplying the monthly water consumption (WC_{mon}, m^3/month) of a product, service or activity from inventory analysis and the WDI_{mon} (Eq. (5)). The differences between C_{mon} and WC_{mon} were that C_{mon} addressed the monthly water consumption status in the research area while WC_{mon} described the consumptive water use of target activities in the research area.

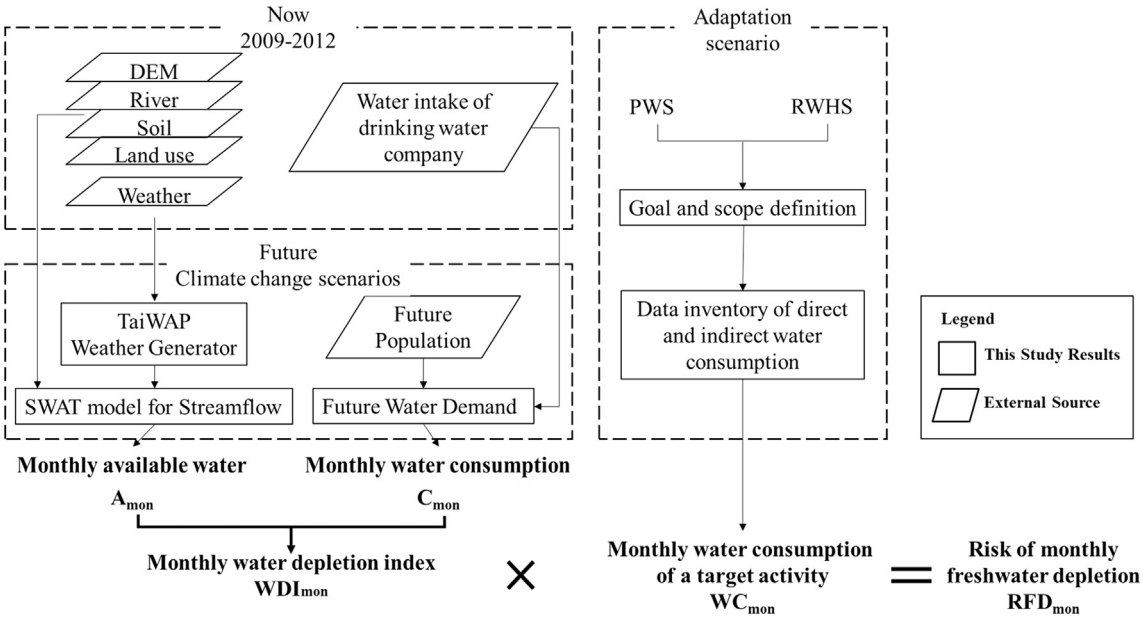

Fig. 1. The framework and data used in the case study. Rectangle described the data that is produced by this study even from running models or calculation. Parallelogram depicted the data that was from external sources and was used as model inputs or parameters in the calculation.

$$RFD_{mon} = WC_{mon} \times WDI_{mon} \quad (5)$$

2.3. Case study

The framework and data used in this study are described in Fig. 1. The case study aims to derive the WDIs of Taipei under different time periods and discuss whether the dynamic concept is necessary. Therefore, the first part of the case study is to calculate current WDIs and future WDIs of Taipei. The former used historical statistical data (2009–2012) and the latter used the prediction data from TaiWAP and SWAT.

In order to demonstrate how the WDIs can support water resource management, we then applied the calculated WDIs to perform a comparative analysis of a potable water system (PWS) and an adaptation measure – an RWHS – in a building by quantifying their risk of freshwater depletion. In the second part of the case study, the spatial scale is a building. And the direct and indirect water consumption of PWS and RWHS was inventoried with defined scope (see Section 2.3.2 Adaptation scenarios).

2.3.1. Spatial description

The research area (water consumer), Taipei, is a highly developed area that is home to many commercial and residential activities. The water supplied to Taipei mainly comes from the Feitsui Reservoir and the streamflow in the Water Quality and Quantity Protection Area. Their relative location is shown in Fig. 2. During 2009–2012, the average annual water withdrawal from the watershed is 868,116,943 m^3. In order to get actual C_{mon} and A_{mon}, we assume that water is withdrawn upstream of the watershed and directly transmitted to potable water treatment plants in the city through pipes. Therefore, C_{mon} is calculated on the basis of Taipei (Yellow area in Fig. 2) and A_{mon} is the simulated results of the upstream of the Feitsui Reservoir (dark green area- Water Quality and Quantity Protection Area in Fig. 2), suggesting that the points of water consumption and water withdrawal may be different. This approach ensures that the WDIs is not underestimated due to overestimations of availability.

2.3.2. Adaptation scenarios

The system boundary of the PWS includes raw water catchment and treatment, potable water distribution, and water usage in toilet flushing (Fig. S3(a)); on the other hand, the RWHS includes the construction of rainwater catchment, a filter, a rainwater storage tank, a pump, and rainwater distribution for toilet flushing (Fig. S3(b)). The placements of PWS and RWHS in the building are shown in Fig. 3. The functional unit (FU) for the analysis is defined as the provision of sanitation services for 204 people in a 4-story research building at National Taiwan University for one month (light green dot in Fig. 2). Water demand is assumed to be the sum of toilet flushing five times per person per day with 6 L per flush for low-flush toilets; that is, 30 L per person per day. This study also assumes (1) the RWHS has a lifetime of at least 20 years and (2) all of the direct and indirect water consumption leads to water depletion risk in the research watershed.

Three scenarios are designed to estimate RFD_{mon} for the case study site:

S0 (PWS): The potable water system is the business as usual scenario.

S1 (RWHS/X): A combination of the rainwater harvesting system and the potable water system uses the addition of the RWHS to the PWS to substitute 70% of potable water for toilet flushing, with saved potable water available to be supplied for other water consumption needs.

S2 (RWHS/X/I): The rainwater harvesting system includes the same infrastructures as in S1. This scenario additionally includes the construction stage of the RWHS, such as catchment, filter, storage tank, pipes, and pumps.

The data inventories of the three scenarios focused on direct and indirect water consumption from the watershed (Fig. 3). While direct water consumption is water directly used for toilet flushing, indirect water consumption includes electricity and chemical inputs in the PWS and electricity usage and the construction stage in the RWHS. The quantity of direct and indirect water flow and the nodes of water collection, reservation and consumption are also presented in Fig. 3. In the PWS (Fig. 3(a)), direct water for toilet flushing is 184 m^3/month in the research building. Indirect water consumption of water treatment procedure, water distribution (from the water treatment plant to the research building) and pumping (when using water in the research building) is 47.1 m^3/month, 7.3 m^3/month and 11.7 m^3/month, respectively. In the RWHS/X and RWHS/X/I (Fig. 3(b)), water consumption from the PWS accounts for 30% of the total consumption of PWS. Direct use of rainwater for toilet flushing is estimated at 129 m^3/month, which is assumed to be excluded from the water depletion

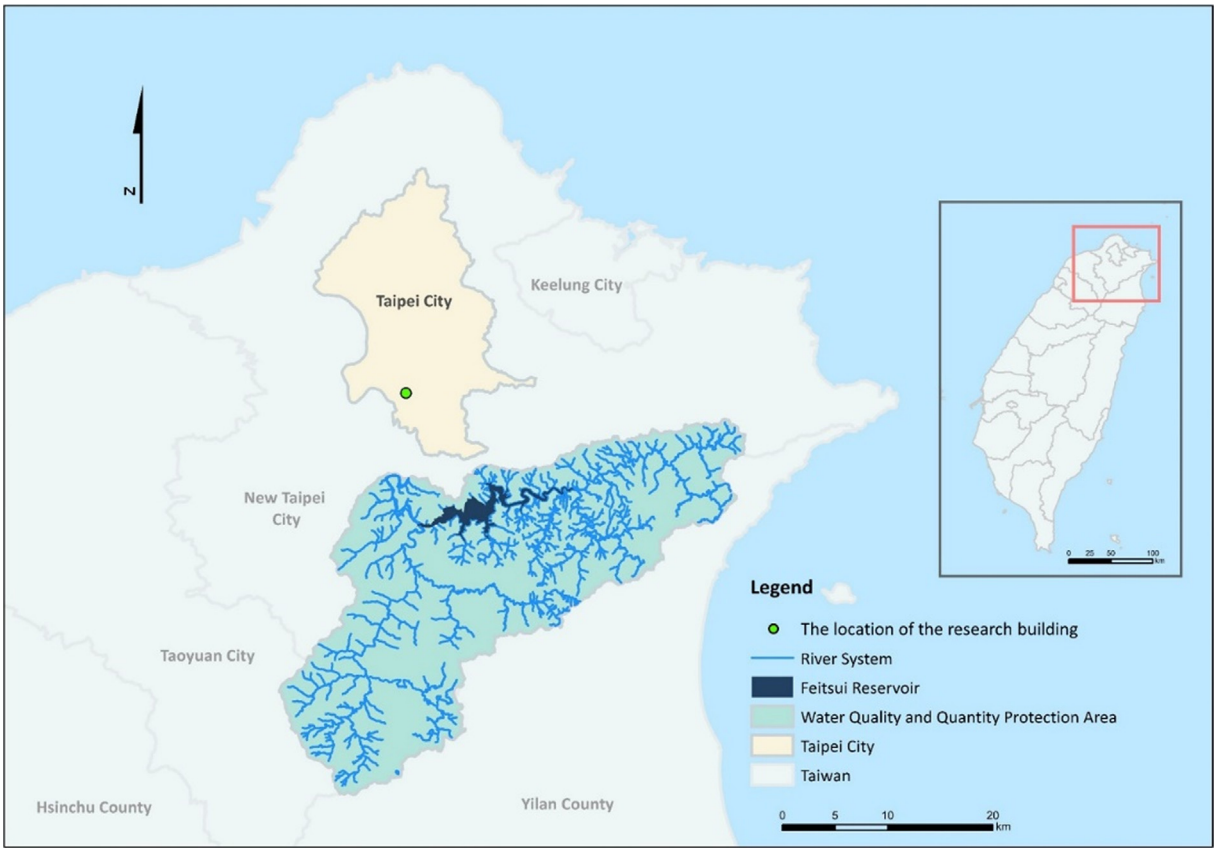

Fig. 2. Spatial description of research area including the research building, Taipei city, Feitsui Reservoir and the water supply watershed.

calculation on the watershed. The indirect water use of RWHS is 0.22 m^3/month for rainwater collection and 8.72 m^3/month for rainwater pumping (when using rainwater in the research building). Detail inventories of the three scenarios are summarized in Tables S5 and S6.

The data on electricity and chemical inputs in PWS were obtained from the Taiwan Water Resources Agency (2013). The inventory of materials used in constructing the RWHS was obtained from the Ecoinvent 3.0 database. The electricity mix data were obtained from the Taiwan Power Company (Taiwan Power Company, 2015). The volume of the storage tanks was modeled by Rain Cycle, which is a continuous mass-balance software that uses the yield after spillage model (Jenkins and Pearson, 1978).

3. Results and discussion

3.1. Dynamic water depletion index

3.1.1. Temporal scale of WDI

Fig. 4 shows the WDIs of the research area at both annual and monthly scales (2009–2012). The WDIs were derived from Eqs. (1)–(3) using historical data. In this study, the AF_{ERF} was adjusted to conform to the result of a WDI of 0.51 for a CTA* of 0.37, which is the threshold between moderate and severe water depletion. The annual WDI determined in this study was 0.732, which was higher than the defined threshold of water depletion and thus indicated severe water depletion. The annual WDI from Berger et al. (2014) is also displayed in the Figs. 4 and S4 for reference. The annual WDI estimated by Berger et al. (2014) was 0.116, which was six times lower than the average WDI calculated in this study. The main differences in the estimations can be attributed to theAF_{ERF} and CTA* in the calculation. In their study, an AF_{ERF} with a value of 40.0 was utilized. This setting was based on the assumptions that the extreme water depletion occurring at CTA* reached 0.25 when the WDI rose to 1 (Fig. S1). This threshold was stricter than that was defined in our study. The lower value of WDI estimated by Berger et al. (2014) might be due to the CTA* was calculated from the modeled annual water consumption and annual availability using WaterGAP2, a global hydrological model. This further suggested that the global hydrological model (or the large spatial scale model, as in Fig. S4) might not be suitable for our research area where regions for water withdrawal and water consumption are not the same.

Using the monthly scale, the maximum WDI_{mon} in April was 0.98, which was approximately four times as high as the minimum WDI_{mon} in October (0.25). Previous research also indicated that monthly or seasonal temporal scales such as high- and low-flow periods are appropriate to depict the water resource status in Taiwan (Lin et al., 2017). This result showed that annual WDI values may not indicate all the water stress that occurs over a year, and thus, such values may mislead water management decision makers (Lin et al., 2017; Scherer et al., 2015); monthly WDI values, however, can be used to provide more specific information to prepare for household water usage and agricultural irrigation in different months (Pfister and Bayer, 2014).

3.1.2. Water depletion index under climate change

Monthly available water (A_{mon}, in Section 2.1.2) in future periods is a key parameter to derive the WDI under climate change in this study. Thus, the monthly precipitation and streamflow under climate change scenarios were simulated and modeled. Fig. S5 presents the results of relative changes in monthly average precipitation and streamflow under climate change scenarios. In general, increased precipitation was simulated during wet seasons (from May to October) and dry seasons (from November to April) in the CSIRO-Mk3.6.0 model. At most, precipitation increased 114% during dry seasons. On the other hand, increased precipitation during wet seasons and decreased precipitation during dry seasons were simulated in the CCSM4 model. These

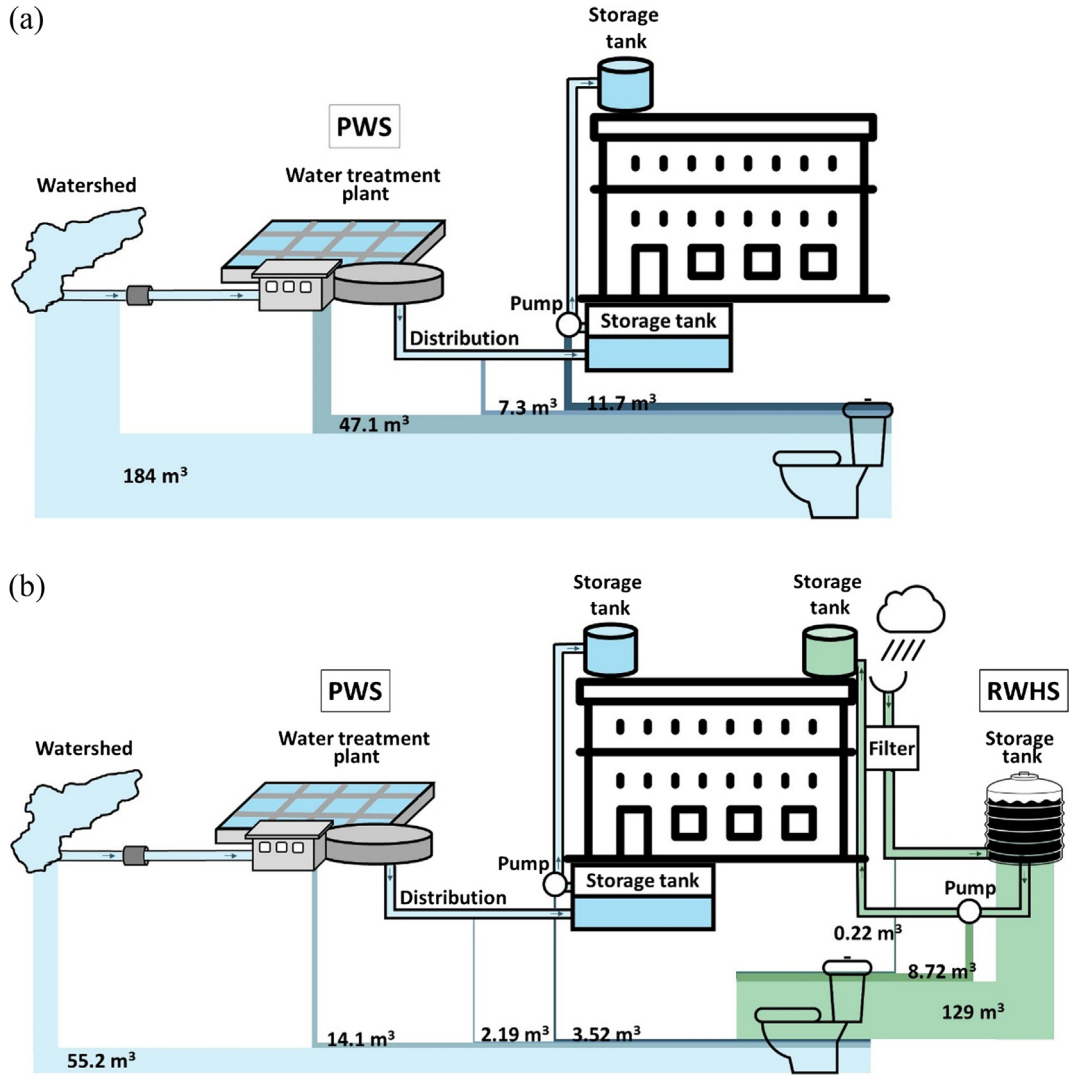

Fig. 3. Water supply system of the research building (for toilet flushing) and the related monthly direct and indirect water flow of (a) a PWS and (b) an RWHS. In Taiwan, most buildings install water storage tanks. Thus, potable water entering a building will first go into an underground storage tank, be pumped to a roof storage tank and then be distributed to end users in the whole building by gravity. These placements were considered in the study.

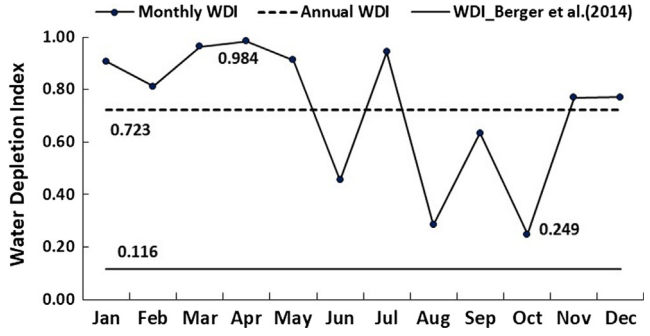

Fig. 4. WDI (2009–2012) at monthly and annual scales in the research area, Taiwan.

simulations indicated that the risk of a strong flood (at most, 136% increased precipitation during the 2090s) and drought (at most, 70% decreased precipitation during the 2070s) might be high in RCP 8.5 scenarios. These results were also validated based on previous studies conducted in northern Taiwan (Yu and Wang, 2009) and showed the suitability of using a monthly scale in the determination of the WDI.

The monthly WDI under climate change were calculated with Eqs. (1)–(3) and the simulated parameters (listed in Supplementary information B). Fig. 5 displays WDI_{mon} in four time periods, under four climate change scenarios and with two GCMs. It was observed that the WDI_{mon} changes considerably. For example, the period of March-May (spring) has higher WDIs, and June-August (summer) has lower WDIs. Out of the four time periods, the 2030s have the highest WDI_{mon} with values being significantly different across the four time periods for all months. The annual WDI derived from average A_{mon}, C_{mon} and SWA_{mon} were also presented in Fig. 5 (dotted lines). The differences between WDI_{mon} under climate change (in Fig. 5) and WDI_{mon} in the corresponding time periods without climate change effect are calculated to examine the influences of climate change on the WDIs. Results of the change in WDI_{mon} is shown in Fig. 6. A significant decrease in WDI_{mon} was observed from June to August, and then an increase in WDI_{mon} from August to October was shown in most time periods and climate change scenarios.

The difference in the characterization factor in time is an essential aspect when considering time in global warming impacts assessment (Pinsonnault et al., 2014). Since WDI_{mon} can also serve as a characterization factor in the life cycle impact assessment (Berger et al., 2014), it can be used to understand its variation in time. Based on the results in Fig. 5, we proposed the concept and application of the dynamic WDI. This “dynamic” concept was also proposed in Levasseur

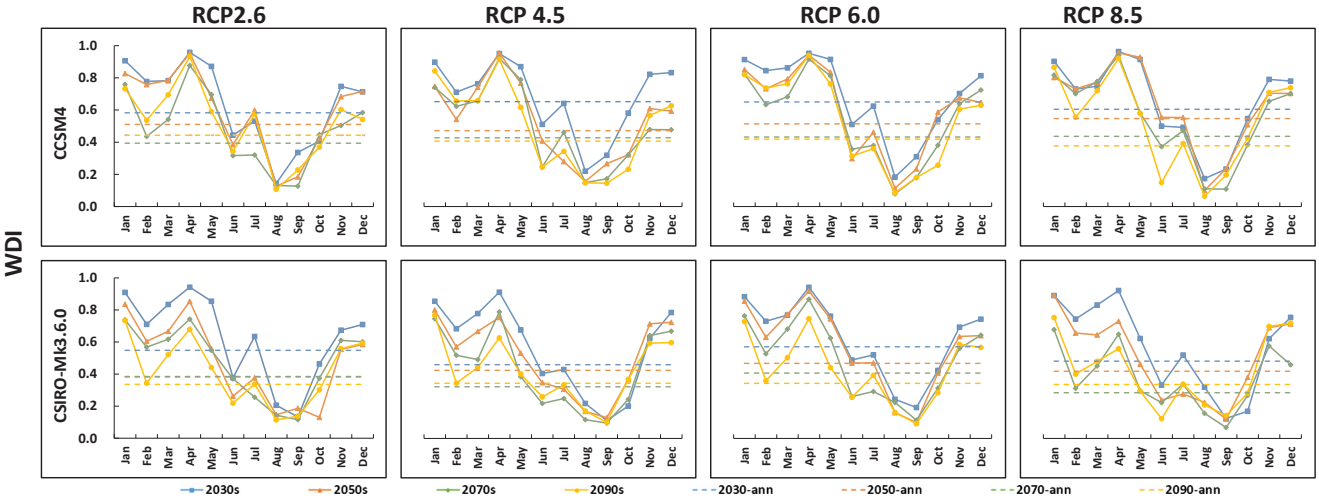

Fig. 5. Monthly WDI_{mon} and annual WDI under climate change scenarios.

et al. (2010) and Pinsonnault et al. (2014) as dynamic life cycle assessment (dynamic LCA). It focused on inclusion of temporal information in every stage of the LCA. Likewise, Collinge et al. (2013) emphasized utilizing time-dependent characterization factors to show the temporal variability of the impacts of an institutional building (a long-lasting infrastructure). Therefore, the dynamicWDI_{mon} is suggested to be coordinated with the appropriate corresponding period when calculating the impacts of water consumption.

3.2. Risk of freshwater depletion in the case study

3.2.1. Current urban water consumption and related impacts

According to the data inventory analysis (Tables S5 and S6), using 1 m^3 potable water in a four-story building in Taipei consumes 1.36 m^3 water, including 1.05 m^3 direct water and 0.31 m^3 indirect water (from raw water treatment, water distribution and water pumping). On the other hand, using 1 m^3 rainwater consumes 0.06 m^3 stressed water due

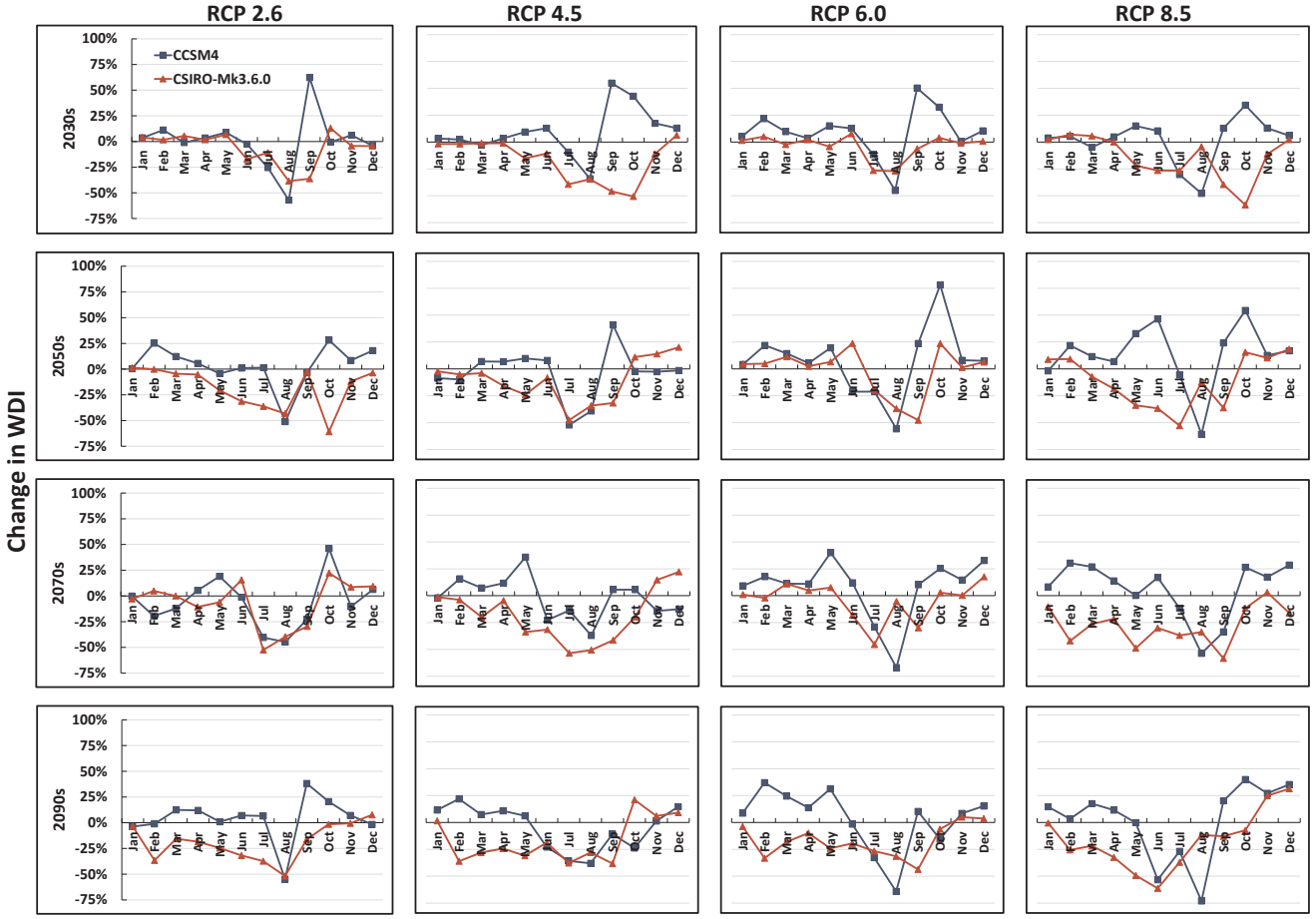

Fig. 6. Relative change in monthly WDI compared with baseline (without climate change effect) under four climate change scenarios (RCP 2.6, RCP 4.5, RCP 6.0, and RCP 8.5) with two GCMs (CCSM4 and CSIRO-Mk3.6.0).

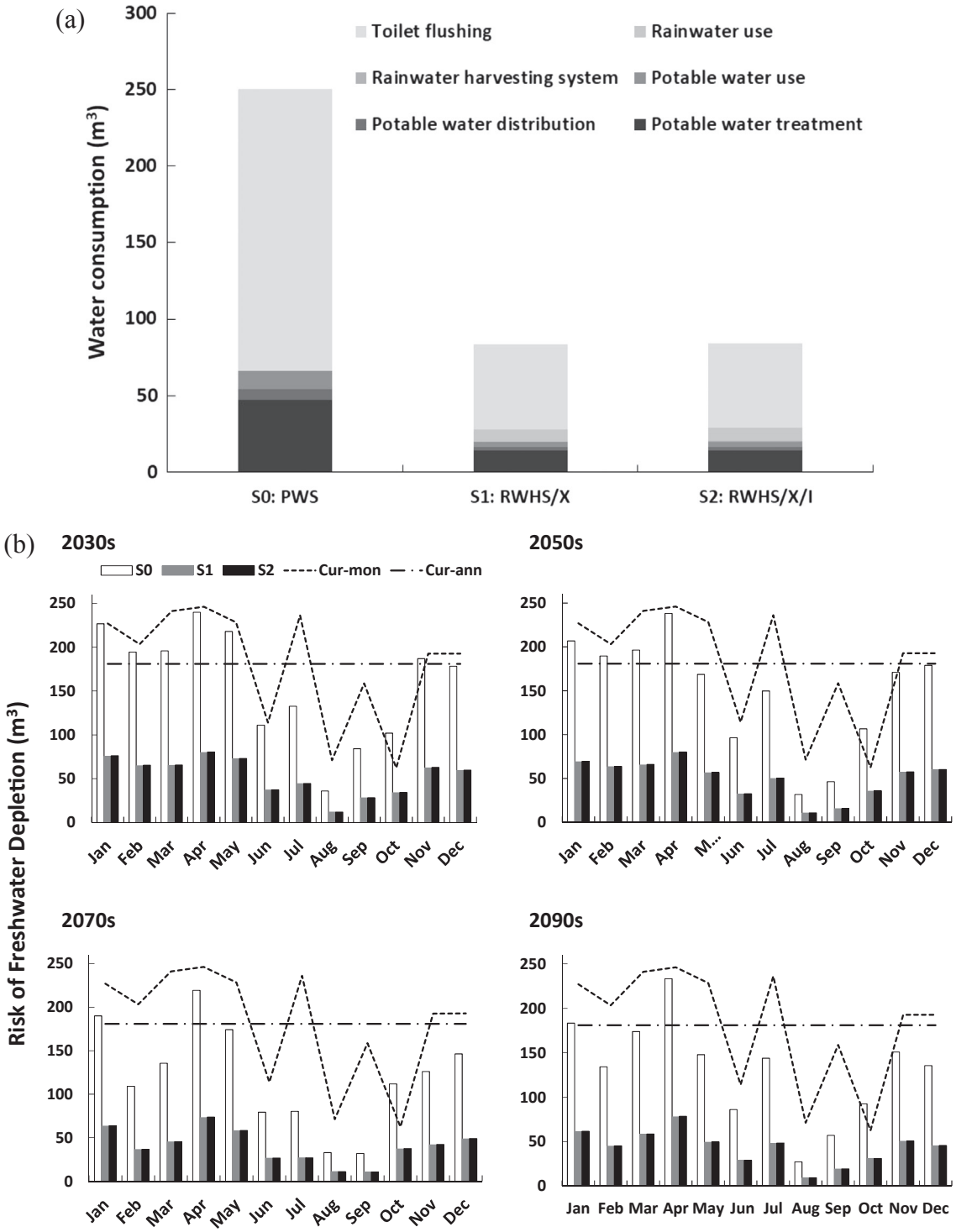

Fig. 7. Water consumption and the related impacts. (a) Water consumption of S0: PWS, S1: RWH/X and S2: RWHS/X/I for toilet flushing. (b) Risk of freshwater depletion (RFD) in the three scenarios under RCP 2.6 with CCSM4 model (dotted line for current monthly and annual risk, respectively). The RFDs of the other RCP scenarios are shown in Fig. S6 and the results are listed in the Supplementary information (B).

to pumping. Considering the construction stage of the RWHS, an additional 0.01 m^3 water was required.

Rainwater reclaimed from the RWHS was assumed to substitute for 70% of the potable water used for toilet flushing. Monthly stressed water consumption of toilet flushing in the research building is shown in Fig. 7(a). Direct rainwater use was excluded from water consumption, as it did not come from the watershed and would not contribute to freshwater depletion. In all of the scenarios, the largest share of water consumption was toilet flushing – the direct potable water use in S0. Moreover, the indirect water use of aluminum oxide used in the potable water purification process was the hotspot in S0, accounting for 26.0% of indirect water consumption. In S1 and S2, indirect water use of electricity for pumping rainwater accounted for 32.4% and 31.6% of indirect water consumption, respectively. This potential impact of the use of electricity for pumping has been validated by Morales-Pinzón et al. (2012). Comparing S0 and S2 (construction of RWHS), the RWHS saved 166.2 m^3 water in toilet flushing every month (including 135.3 m^3 direct water and 30.9 m^3 indirect water). By applying an

RWHS, potable water could be saved and applied to more valuable uses.

By comparing S1 and S2, it seems that the water consumption for the construction of an RWHS is negligible. As shown in Fig. 7(a) and Table S6, the water consumption in the rainwater catchment (including collecting pipe, sand and storage tank) and in the rainwater use stage (including pump, supply pipe and storage tank) are 0.2 m^3 and 0.5 m^3, respectively. These results are due to the relatively long lifespan of an RWHS at 20 years. However, inclusion of the construction stage in the impact assessment is suggested, especially when life cycle energy and resources are required for a long-lasting infrastructure.

3.2.2. Urban water consumption under the influences of climate change

Reduction in water depletion risk (Eq. (5)) was also calculated in this study to demonstrate how dynamic WDI_{mon} results (in Fig. 5) can apply for evaluation of adaptation measures. Fig. 7(b) and Fig. S6 reveal the RFD_{mon} of toilet flushing (dotted line for current monthly and annual risk and colored bars for different scenarios). The differences between the scenarios in Figs. 7(b) and S6 indicated the reduction in RFD_{mon} due to the application of the RWHS. In the RWHS, the risk of freshwater depletion was less fluctuant. The potential of reduction in RFD_{mon} was in the range of 17.9 m^3 to 159.3 m^3 when the RWHS was used. Vialle et al. (2015) conducted an RWHS analysis with Boulay's water stress indicator (Boulay et al., 2011) and showed a similar result in which an RWHS was 0.71 L-eq lower than a PWS with the functional unit of 30 L of water for toilet flushing per day.

Although the environmental performance of the RWHS alone seemed to be poorer than that of PWS (Anand and Apul, 2011; Crettaz et al., 1999), the RWHS did show more water savings than the PWS when the impacts of water resource depletion were considered (Vialle et al., 2015). Additionally, the water saved by the RWHS is due to not only the saving of stressed water from the watershed but also to the reduction in chemicals and energy used for potable water treatment.

3.3. Limitations

The variation of WDI is strongly affected by water consumption (C_{mom}) and water availability related factors. In this research, the temporal and spatial resolution of WDI_{mon} with simulated available water (A_{mon}) were improved. As a result, a slight decrease in WDI_{mon} was observed for future scenarios (Fig. 5), which was partly due to the increase in future available water from projected precipitation and streamflow under the influence of climate change (Fig. S6). It is worth mentioning that increase in rainwater quantity does not guarantee the increase of water availability, as the rainwater usually accompanies with high turbidity from seriously erosion nearby the watershed (Fakour et al., 2016). Besides, it is difficult to catch the high streamflow in a short duration, particularity because of the terrain characteristics of short rivers in Taiwan.

On the other hand, C_{mom} is primarily estimated based on the projection of population in this research. The water consumption per capita per day was assumed remaining as it is at present, which neglected the potential of future advancement of water management strategies and technologies. If the quantity of water saving is large enough to change the distribution of regional water resources, the potential of water conservation is suggested to be included in the C_{mom} estimation. For example, a water conservation research in California reported that the potential of water reduce use could reach to 34% from residential indoor and outdoor use, commercial use and industrial use (Gleick et al., 2003). In this case, the savings would be taken into consideration when calculating future WDIs. Therefore, WDI_{mon} could be further improved with refined availability water considering water quality issue as well as contribution of water conservation.

4. Conclusions

This study proposed an approach for constructing a dynamic WDI under climate change scenarios, using modeled monthly available water and water consumption. The WDI_{mon} can serve as a characterization factor in the life cycle impact assessment, in order to understand its variation in impact results over time. This index can also be applied to determine whether applying different WDI_{mon} is necessary when assessing impacts of water consumption.

In this case study, parameters for calculating WDI_{mon} in Taipei, Taiwan was derived as follows: regional watershed data and projected precipitation. The abovementioned parameters were applied to the hydrological model for simulating available water with consideration of the reservoir inflow data as the surface water stock. In addition, the actual water intake data for potable water facilities were used to represent water consumption, instead of using the simulated data.

Impact assessment on water consumption of an RWHS at a four-story-building scale was conducted to demonstrate the applicability of dynamic characterization factor. The results showed that RWHS could save potable water for more valuable uses. With the dynamic WDI_{mon}, the impact results can show the monthly change of risk of water depletion with different time periods, which could provide more information about the consequence of water consumption.

The use of dynamic WDI in this study facilitates the understanding of its monthly variation within a year due to the geographical or climate condition. It is also worth noting that WDI can be applied to any defined temporal scales such as in season. The changes in WDI for future scenarios could be attributed to the influence of climate change. Therefore, it is suggested that the dynamicWDI_{mon}should be coordinated with the appropriate corresponding period when calculating the impacts of water consumption, especially when assessing water-related adaption strategies in water consumption hot spots, in response to climate change.

Acknowledgments

This work was financially supported by National Taiwan University from Excellence Research Program – Core Consortiums (NTUCCP – 106R890909 and 107L891309) within the framework of the Higher Education Sprout Project by the Ministry of Education (MOE) in Taiwan.

Appendix A. Supplementary data

Additional modeling details, simulation results, inventory data and RFD estimation are included in the Supporting information.

Supplementary data to this article can be found online at https://doi.org/10.1016/j.jhydrol.2019.02.032.

References

Acreman, M., Dunbar, M., Hannaford, J., Mountford, O., Wood, P., Holmes, N., Cowx, I.A.N., et al., 2008. Developing environmental standards for abstractions from UK rivers to implement the EU Water Framework Directive/Développement de standards environnementaux sur les prélèvements d'eau en rivière au Royaume Uni pour la mise en œuvre de la directive cadre sur l'eau de l'Union Européenne. Hydrol. Sci. J. 53 (6), 1105–1120. https://doi.org/10.1623/hysj.53.6.1105.

Anand, C., Apul, D.S., 2011. Economic and environmental analysis of standard, high efficiency, rainwater flushed, and composting toilets. J. Environ. Manage. 92 (3), 419–428. https://doi.org/10.1016/j.jenvman.2010.08.005.

Belmeziti, A., Coutard, O., de Gouvello, B., 2014. How much drinking water can be saved by using rainwater harvesting on a large urban area? Application to Paris agglomeration. Water Sci. Technol. 70 (11), 1782–1788. https://doi.org/10.2166/wst.2014.269.

Berger, M., Van Der Ent, R., Eisner, S., Bach, V., Finkbeiner, M., 2014. Water accounting and vulnerability evaluation (WAVE): Considering atmospheric evaporation recycling and the risk of freshwater depletion in water footprinting. Environ. Sci. Technol. 48 (8), 4521–4528. https://doi.org/10.1021/es404994t.

Boulay, A.M., Bulle, C., Bayart, J.B., Deschenes, L., Margni, M., 2011. Regional characterization of freshwater use in LCA: Modeling direct impacts on human health. Environ. Sci. Technol. 45 (20), 8948–8957. https://doi.org/10.1021/es1030883.

Collinge, W.O., Landis, A.E., Jones, A.K., Schaefer, L.A., Bilec, M.M., 2013. Dynamic life cycle assessment: framework and application to an institutional building. Int. J. Life Cycle Assess. 18 (3), 538–552. https://doi.org/10.1007/s11367-012-0528-2.

Crettaz, Jolliet, Cuanillon, Orlando, 1999. Life cycle assessment of drinking water and rain water for toilets flushing. Aqua 48 (3), 73–83. https://doi.org/10.1046/j.1365-2087.1999.00134.x.
Fakour, H., Lo, S.L., Lin, T.F., 2016. Impacts of Typhoon Soudelor (2015) on the water quality of Taipei. Taiwan. Sci. Rep. 6, 25228.
Fonseca, C.R., Hidalgo, V., Díaz-Delgado, C., Vilchis-Francés, A.Y., Gallego, I., 2017. Design of optimal tank size for rainwater harvesting systems through use of a web application and geo-referenced rainfall patterns. J. Clean. Prod. 145, 323–335. https://doi.org/10.1016/j.jclepro.2017.01.057.
Gleick, P.H., Haasz, D., Henges-Jeck, C., Srinivasan, V., Wolff, G., Cushing, K.K., Mann, A., 2003. Waste Not, Want Not: The Potential for Urban Water Conservation in California. Pacific Institute for Studies in Development. Environment, and Security, California, USA.
Godskesen, B., Hauschild, M., Rygaard, M., Zambrano, K., Albrechtsen, H.J., 2013. Life-cycle and freshwater withdrawal impact assessment of water supply technologies. Water Res. 47 (7), 2363–2374. https://doi.org/10.1016/j.watres.2013.02.005.
Hoekstra, A.Y., Mekonnen, M.M., Chapagain, A.K., Mathews, R.E., Richter, B.D., 2012. Global monthly water scarcity: Blue water footprints versus blue water availability. PLoS One 7 (2), e32688. https://doi.org/10.1371/journal.pone.0032688.
Hsu, H. H., C. Chou, Y. C. Wu, M. M. Lu, C. T. Chen, & Y. M. Chen (2011), Climate change in Taiwan: Scientific report 2011 (Summary), edited by N. S. Council, p. 67, Taipei, Taiwan.
IPCC, 2014. The fifth assessment report (AR5). The Intergovernmental Panel on Climate Change, Geneva, Switzerland.
Jenkins, D., Pearson, F., 1978. Feasibility of rainwater collection systems in California. Rep., Californian Water Resources Center. University of California.
Levasseur, A., Lesage, P., Margni, M., Deschênes, L., Samson, R., 2010. Considering Time in LCA: Dynamic LCA and Its Application to Global Warming Impact Assessments. Environ. Sci. Technol. 44 (8), 3169–3174. https://doi.org/10.1021/es9030003.
Li, Y., Huang, Y., Ye, Q., Zhang, W., Meng, F., Zhang, S., 2018. Multi-objective optimization integrated with life cycle assessment for rainwater harvesting systems. J. Hydrol. 558, 659–666.
Lin, C.-C., Lin, J.-Y., Lee, M., Chiueh, P.-T., 2017. Sector-wise midpoint characterization factors for impact assessment of regional consumptive and degradative water use. Sci. Total Environ. 607, 786–794. https://doi.org/10.1016/j.scitotenv.2017.07.026.
Liu, C.-M., Chen, J.-W., Hsieh, Y.-S., Liou, M.-L., Chen, T.-H., 2015. Build sponge eco-cities to adapt hydroclimatic hazards. In: Handbook of Climate Change Adaptation, pp. 1997–2009.
Liu, T.-M., Tung, C.P., Ke, K.Y., Chuang, L.H., Lin, C.Y., 2009. Application and development of a decision-support system for assessing water shortage and allocation with climate change. Paddy Water Environ. 7 (4), 301. https://doi.org/10.1007/s10333-009-0177-7.
Morales-Pinzón, T., Lurueña, R., Rieradevall, J., Gasol, C.M., Gabarrell, X., 2012. Financial feasibility and environmental analysis of potential rainwater harvesting systems: a case study in Spain. Conserv. Recycl. 69, 130–140. https://doi.org/10.1016/j.resconrec.2012.09.014.
Moriasi, D.N., Arnold, J.G., Van Liew, M.W., Bingner, R.L., Harmel, R.D., Veith, T.L., 2007. Model evaluation guidelines for systematic quantification of accuracy in watershed simulations. Trans. ASABE 50 (3), 885–900.
Núñez, M., Pfister, S., Vargas, M., Antón, A., 2015. Spatial and temporal specific characterisation factors for water use impact assessment in Spain. Int. J. Life Cycle Assess. 20 (1), 128–138. https://doi.org/10.1007/s11367-014-0803-5.
Neitsch, S.L., Arnold, J.G., Kiniry, J.R., Williams, J.R., 2009. Soil and water assessment tool theoretical documentation: Version 2009 Rep., 618 pp. Texas A&M Universuty System.
Pandey, D.N., Gupta, A.K., Anderson, D.M., 2003. Rainwater harvesting as an adaptation to climate change. Curr. Sci. 85 (1), 16.
Pfister, S., Bayer, P., 2014. Monthly water stress: Spatially and temporally explicit consumptive water footprint of global crop production. J. Clean. Prod. 73, 52–62. https://doi.org/10.1016/j.jclepro.2013.11.031.
Pfister, S., Koehler, A., Hellweg, S., 2009. Assessing the environmental impacts of freshwater consumption in LCA. Environ. Sci. Technol. 43 (11), 4098–4104. https://doi.org/10.1021/es802423e.
Pinsonnault, A., Lesage, P., Levasseur, A., Samson, R., 2014. Temporal differentiation of background systems in LCA: relevance of adding temporal information in LCI databases. Int. J. Life Cycle Assess. 19 (11), 1843–1853. https://doi.org/10.1007/s11367-014-0783-5.
Sample, D.J., Liu, J., 2014. Optimizing rainwater harvesting systems for the dual purposes of water supply and runoff capture. J. Clean. Prod. 75 (Supplement C), 174–194. https://doi.org/10.1016/j.jclepro.2014.03.075.
Scherer, L., Venkatesh, A., Karuppiah, R., Pfister, S., 2015. Large-scale hydrological modeling for calculating water stress indices: implications of improved spatio-temporal resolution, surface-groundwater differentiation, and uncertainty characterization. Environ. Sci. Technol. 49 (8), 4971–4979. https://doi.org/10.1021/acs.est.5b00429.
Soligno, I., Ridolfi, L., Laio, F., 2017. The environmental cost of a reference withdrawal from surface waters: definition and geography. Adv. Water Resour. 110, 228–237. https://doi.org/10.1016/j.advwatres.2017.10.016.
Taiwan Water Resources Agency, 2013. Water footprint accounting of tap water. Ministry of Economic Affairs, Taipei, Taiwan.
Taiwan Water Resources Agency, 2014. Mechanism development and strategies implementation of environmental flows under climate change (1/2), MOEAWRA1030250. Ministry of Economic Affairs, Taipei, Taiwan.
Taiwan Power Company (2015), Annual power generation, Taipei, Taiwan. Retrieved from http://www.taipower.com.tw/tc/page.aspx?mid=212&cid=120&cchk=f3a1b1e0-03e5-45fa-b72e-b28c5cb94f37 (accessed 2015/12/31).
The World Economic Forum (2016), The global risks report 2016: 11th edition, Geneva, Switzerland. Retrieved from http://www3.weforum.org/docs/GRR/WEF_ GRR16.pdf.
Tung, C.-P., Liu, T.-M., Chen, S.-W., Ke, K.-Y., Li, M.-H., 2014. Carrying capacity and sustainability appraisals on regional water supply systems under climate change. Br. J. Environ. Clim. Change 1 (2), 18.
UNEP (2008), Vital water graphics – An overview of the state of the world's fresh and marine waters, The United Nations Environment Programme, Nairobi, Kenya. Retrieved from http://wedocs. unep.org/bitstream/handle/20.500.11822/20624/Vital_water_graphics.pdf?sequence=1&isAllowed=y.
Vialle, C., Busset, G., Tanfin, L., Montrejaud-Vignoles, M., Huau, M.C., Sablayrolles, C., 2015. Environmental analysis of a domestic rainwater harvesting system: a case study in France. Conserv. Recycl. 102, 178–184. https://doi.org/10.1016/j.resconrec.2015.07.024.
Vieira, A.S., Beal, C.D., Ghisi, E., Stewart, R.A., 2014. Energy intensity of rainwater harvesting systems: a review, Renew. Sust. Energ. Rev. 34 (Supplement C), 225–242. https://doi.org/10.1016/j.rser.2014.03.012.
Yu, P.-S., Wang, Y.-C., 2009. Impact of climate change on hydrological processes over a basin scale in northern Taiwan. Hydrol. Process. 23 (25), 3556–3568. https://doi.org/10.1002/hyp.7456.